POET: Prompt Offset Tuning for Continual Human Action Adaptation

Prachi Garg[1], K J Joseph[3], Vineeth N Balasubramanian[3], Necati Cihan Camgoz[2], Chengde Wan[2], Kenrick Kin[2], Weiguang Si[2], Shugao Ma[2], and Fernando De La Torre[1]

[1] Carnegie Mellon University, USA
[2] Meta Reality Labs
[3] Indian Institute of Technology, Hyderabad

Abstract. As extended reality (XR) is redefining how users interact with computing devices, research in human action recognition is gaining prominence. Typically, models deployed on immersive computing devices are static and limited to their default set of classes. The goal of our research is to provide users and developers with the capability to personalize their experience by adding new action classes to their device models continually. Importantly, a user should be able to add new classes in a low-shot and efficient manner, while this process should not require storing or replaying any of user's sensitive training data. We formalize this problem as privacy-aware few-shot continual action recognition. Towards this end, we propose *POET: Prompt-offset Tuning*. While existing prompt tuning approaches have shown great promise for continual learning of image, text, and video modalities; they demand access to extensively pretrained transformers. Breaking away from this assumption, POET demonstrates the efficacy of prompt tuning a significantly lightweight backbone, pretrained exclusively on the base class data. We propose a novel spatio-temporal learnable prompt offset tuning approach, and are the first to apply such prompt tuning to *Graph Neural Networks*. We contribute two new benchmarks for our new problem setting in human action recognition: (i) NTU RGB+D dataset for activity recognition, and (ii) SHREC-2017 dataset for hand gesture recognition. We find that POET consistently outperforms comprehensive benchmarks. [4]

Keywords: 3D Skeleton Activity Recognition · Extended Reality (XR) · Continual Learning · Prompt Tuning.

1 Introduction

A key input modality to virtual, augmented and mixed reality (often together termed as extended reality, XR) devices today is through recognizing human

[4] Source Code at https://github.com/humansensinglab/POET-continual-action-recognition

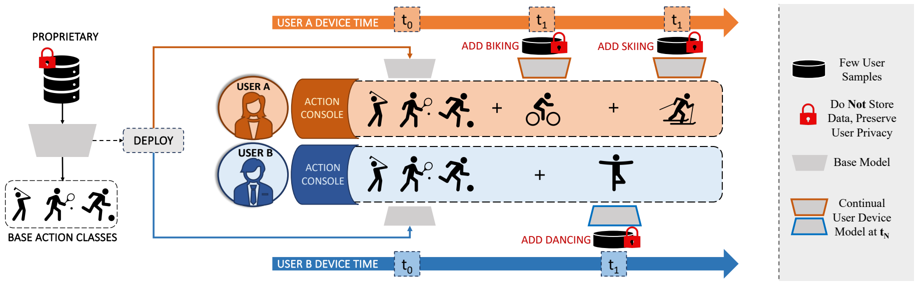

Fig. 1: Proposed POET method **continually adapts** skeleton-based human action recognition models pretrained on a pre-defined set of categories **to new user categories with few training examples**. Users can thus expand the capabilities of XR systems with novel action classes by providing a few examples of each new class. We discard the user-sensitive data as soon as the model is updated on the new categories.

activity and hand gestures based on body and hand pose estimates. Recognizing human actions[5] facilitates seamless user interactions in head-mounted XR devices such as the Meta Quest 3 and Apple Vision Pro. If the provided action recognition models are static, then developers and users are limited to a pre-defined set of action categories. With the growing use of such devices in new contexts and the increasing demand for personalized technology delivery, there is an impending need to enable the action recognition models in such systems to adapt and learn new user actions over time. Defining their own action categories allows users to customize their experience and expand the functionality of their XR devices. Addressing this need is the primary objective of this work.

Adapting human action models to new user categories over time faces a few challenges. Firstly, the model must be capable of learning new actions with minimal amount of training data so users can add new classes by providing just a few training examples per class. Secondly, due to the increasing use of XR devices for personal assistance, there is a need for privacy preservation in user action recognition-based pipelines [2,14]. Hence, the adaptation of such action recognition models to new user categories must also be 'data-free', i.e., it cannot store and replay previously seen user training data in subsequent continual sessions. Considering these requirements, we leverage the recent success of 'data-free' prompt-based learning [49] and propose a new spatio-temporal prompt offset tuning approach to efficiently adapt the default model without finetuning.

Human action recognition systems are moving to skeleton-based approaches, especially in applications that require low-shot action recognition capabilities such as medical action recognition [27,56]. Skeletons offer a robust and compact alternative to videos in such low-shot regimes, due to their relatively low dimensionality and lesser variance under background conditions. While there have been a wide variety of efforts in skeleton-based human action recognition over the years [36,52,53], there have been fewer efforts on adapting such models to newer user categories. Efforts like [1,22] attempted to continually learn new user

[5] We use human action as an umbrella term for both hand gesture and body activity in this work for ease of presentation.

categories over time in skeleton-based human action recognition, but relied on fully-supervised data for the new classes. On the other hand, few-shot learning works [27, 46, 56] adapt a pretrained skeleton-based action recognition model to new data, but without explicitly retaining past categories. In this work, we seek to learn new user categories in trained human action models with *very few labeled samples* for the new classes, while being *data-free* (not storing samples from previously trained categories). Fig 1 summarizes our overall objective. One could view our setting as privacy-aware few-shot continual learning for skeleton-based action recognition.

To this end, we propose a prompt offset tuning methodology that can be integrated with existing backbone architectures for skeleton-based human action recognition. Our learnable (soft) prompts are selected from a shared knowledge pool of prompts based on an input instance dependent attention mechanism. In particular, we propose prompt selection using an ordered query-key matching that enables a temporal *prompt* frame order selection consistent with the input instance. We show that such an approach allows us to learn new user categories without having to store data from past classes, without overwriting the pre-existing categories. To the best of our knowledge, this is the first effort on leveraging prompt tuning for skeleton-based models, as well as on spatio-temporal prompt selection and tuning.

Our key contributions are summarized below:

- We formalize a novel problem setting which continually adapts human action models to new user categories over time, in a privacy aware manner.
- To address this problem, we propose a novel spatio-temporal Prompt OffsEt Tuning methodology (POET). In particular, it is designed to seamlessly plug-and-play with a pretrained model's input embedding, without any significant architectural changes.
- Our comprehensive experimental evaluation on two benchmark datasets brings out the efficacy of our proposed approach.

2 Related Works

2.1 Prompt Tuning

The idea of prompting, as it originated from Large Language Models (LLMs), is to include additional information, known as a text prompt, to condition the model's input for generating an output relevant to the prompt. Instead of applying a discrete, pre-defined 'hard' language prompt token, *prompt and prefix tuning* [20, 23] formalized the concept of applying 'soft prompts' to the input. A set of learnable parameters are prepended (concatenated) to the input text and trained along with the classifier while keeping the backbone parameters frozen. Similar to prompt tuning of LLMs, recent works have popularized prompt tuning of ViTs [16] as an effective way of adapting large pretrained models to downstream tasks [49, 57]. However, it remains unexplored and undefined (to the best of our knowledge) for *non-transformer* architectures such as GNNs.

2.2 Prompt Tuning for Continual Learning

Prompt tuning provides a simple and cost-effective way of learning task-specific signal condensed into 'soft prompts'. For continual learning, training a set of prompts for each sequential task provides a natural alternative to storing privacy violating exemplars and replaying them. Training task-specific prompts for each sequential task is straightforward when authors assume access to task identity at both train and inference time, like in Progressive Prompts [34]. However, if task identity is unavailable at inference, the model will not know which task's prompts or classifier to use for evaluating a test sample. In this respect, S-prompts [47] and A-la-carte prompt tuning (APT) [4] learn an independent set of prompts for each domain/task and employ a KNN-based search for domain/task identity at test time. Since these methods learn stand-alone prompts for every task, the prompt feature space is task-specific, and there is no forgetting of old knowledge when learning new tasks (by design). At the same time however, these 'no forgetting' prompts *cannot share knowledge* across tasks.

This leads to another ideology for continual prompt tuning, i.e., treat each prompt unit as being a part of a larger **shared (knowledge) pool** of prompts. Then the desired number of prompt units can be selected from the pool, conditioned on the input instance itself [41,48,49]. Given the scarcity of new data in our setting, we hypothesize that sharing of knowledge will benefit new tasks and draw inspiration from this line of works. Most recently, Adaptive Prompt Generator (APG) [42] challenges the intensive ImageNet21K pre-training assumption as it prompts a ViT pretrained only on the continual benchmark's base class data (similar to us). However, they use replay and knowledge distillation-style 'anti-forgetting learning', in addition to using prompts. Even though our backbone is trained only on the base classes, we propose a **simple prompt tuning-only** strategy to counter forgetting. This implies that a prompt strategy is all we need to continually add new action semantics in a few-shot manner.

2.3 Few-Shot Class Incremental Learning

FSCIL is a challenging continual learning setting where a model overfits to new classes, with the simultaneous heightened (often complete) forgetting of old knowledge as soon as the base model is fine-tuned on few-shot data [10,43]. Since the backbone feature extractor is the only source of previously seen knowledge, if it is updated, knowledge is lost forever. Typically, existing works decouple the learning of (backbone) feature representations from the classifier by *learning* the model *only on the base data* and relying on non-parametric class-mean classifiers for classification in subsequent steps [13,31,55]. This leads to a feature-classifier misalignment issue [32, 51] because new class prototypes are extracted from a backbone representation trained only on the base classes. We hypothesize that optimizing input prompt vectors along with a dynamically expanding parametric classifier on top of a frozen backbone can alleviate this misalignment issue. Our work not only provides a fresh perspective into FSCIL, but to our best knowledge is also the only work not designed for and evaluated on image benchmarks.

3 Preliminaries

Skeleton Action Recognition Using Graph Representations. Our input $\mathbf{X} \in \mathbb{R}^{T \times J \times 3}$ is a video sequence of T frames, each frame containing J joints of the human body (25 joints) or hand skeleton (22 joints) in 3D Cartesian coordinate system. Such a skeleton action sequence is naturally represented as a graph topology $G = \{\mathcal{V}, \mathcal{E}\}$ with $\mathcal{V}$ vertices and $\mathcal{E}$ edges. Graphs are modeled using Graph Neural Networks (GNNs) [12], which can either be sparse graph convolutional networks (GCN) or fully connected graph transformers (GT). Our main model (a GNN) is defined as $f(\mathbf{X}) = f_c \circ f_g \circ f_e(\mathbf{X})$ (as also shown in Fig. 2). Input $\mathbf{X}$ is first passed through an input embedding layer f_e to get an embedding of human joints $\mathbf{X_e} = f_e(\mathbf{X}), \mathbf{X_e} \in \mathbb{R}^{T \times J \times C_e}$, with feature dimension C_e. $\mathbf{X_e}$ is further passed to a graph feature extractor f_g composed of a stack of convolutional layers (in GCNs) or attention layers (in GTs), and finally a classifier f_c which predicts the action class label $\mathbf{y}$. In POET, we propose to attach learnable parameters $\mathbf{P_T}$ (called prompt offsets) to the embedding $\mathbf{X_e}$.

Problem Definition. Given a default (pre)trained model deployed on a user's device, we would like to extend this model to new action classes over T subsequent user sessions (also called tasks) $\{\mathcal{US}^{(1)}, ..., \mathcal{US}^{(T)}\}$[6]. In each user session $\mathcal{US}^{(t)}$, the model learns a dataset $\mathcal{D}^{(t)} = (\mathbf{X}_i^t, \mathbf{y}_i^t)_{i=1}^{|\mathcal{D}^{(t)}|}$ of skeleton action sequence and label pairs provided by the user, $\mathbf{X}_i^t \in \mathbb{R}^{T \times J \times 3}$, $y_i^t \in \mathbb{R}^{\mathcal{Y}^{(t)}}$. In each session, the user typically provides a few training instances F (e.g. $F \leq 5$) for each of the N new classes being added, such that $|\mathcal{D}^{(t)}| = NF$. The base (default) model's session $\mathcal{UB}^{(0)}$ is assumed to have a large number of default action classes $\mathcal{Y}^{(0)}$ trained on sufficient data $\mathcal{D}^{(0)}$, which is most often proprietary and cannot be accessed in later user sessions. In each session, the user adds new action classes such that, $\mathcal{Y}^{(t)} \cap \mathcal{Y}^{(t')} = \emptyset, \forall t \neq t'$[7]. Due to the aforementioned privacy constraints, in any training session $\mathcal{US}^{(t)}$, the model has access to only $\mathcal{D}^{(t)}$; after training this data is made inaccessible for use in subsequent sessions (no exemplar or prototypes stored). After training on every new session $\mathcal{US}^{(t)}$, the model is evaluated on the test set of all classes seen so far $\cup_{i=0}^{t} \mathcal{Y}^{(i)}$. The challenge is to alleviate forgetting of old classes while not overfitting to the user-provided new class samples. One could view our setting as privacy-aware few-shot continual action recognition, a problem of practical relevance in human action recognition – which has not received adequate attention.

4 Methodology: Prompt Offset Tuning (POET)

Overview. We propose to prompt tune a base GNN model $f(.)$ by prompts $\mathbf{P_T}$ to address our overall objective. As shown in Fig. 3, for each input instance $\mathbf{X}$, corresponding prompts $\mathbf{P_T}$ are selected from a pool of prompt parameters, using an input-dependent query and key attention mechanism. The selected prompts

[6] User sessions may be spaced at arbitrary time intervals.

[7] We make this assumption considering this is a first of such efforts; allowing for overlapping action classes and users to 'update' older classes would be interesting extensions of our proposed work.

are added to the input feature embedding (and hence the term '*prompt offsets*'), before forwarding to the feature extractor and classifier (shown in Fig. 2).

To this end, our method, POET uses the same number of prompts as the number of temporal frames in the input, to maintain temporal consistency between the prompt and the input. Focusing solely on prompt offsets allows us to adapt the model to subsequent user sessions without having to update the input embeddings or the feature extraction backbone. Our prompt selection mechanism is learnable and trained along with the classifier to make this method simple and efficient.

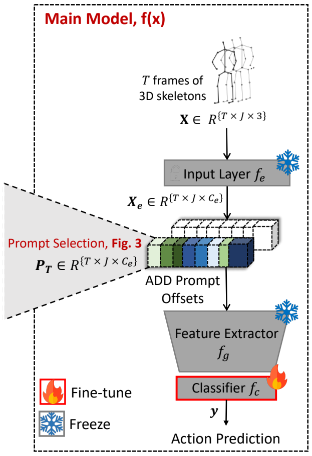
Main Model, f(x)
T frames of 3D skeletons
$\mathbf{X} \in R^{\{T \times J \times 3\}}$
Input Layer f_e
$\boldsymbol{X_e} \in R^{\{T \times J \times C_e\}}$
Prompt Selection, Fig. 3
$\boldsymbol{P_T} \in R^{\{T \times J \times C_e\}}$
ADD Prompt Offsets
Feature Extractor f_g
Classifier f_c
$\boldsymbol{y}$
Action Prediction
Fine-tune
Freeze

Fig. 2: POET: Prompt-offset Tuning proposes to offset the input feature embedding $\mathbf{X_e}$ of the main model by learnable prompt parameters $\mathbf{P_T}$ for privacy-aware few-shot continual action recognition. We explain prompt selection mechanism in Fig. 3.

What are Prompt Offsets? Learnable (or soft [20]) prompts are parameter vectors in a continuous space which are optimized to adapt the pretrained frozen backbone f_g to each continual task. We define our spatio-temporal prompt offsets $\mathbf{P_T}$ as a set of T prompts (same in number as skeletal frames in input), each prompt $\boldsymbol{P_i}$ having length equal to the number of joints in a frame J and feature dimension same as input feature embedding $\mathbf{X_e}$, i.e., $\boldsymbol{P_i} \in \mathbb{R}^{J \times C_e}$.

Existing prompt tuning efforts, for example in image classification, focus on concatenating learnable prompts to the input token sequence in transformer architectures [16, 20]. Even though transformers can be generalized to graphs [7,11,29], it is non-trivial to attach prompts to a GNN. This is because transformers can be viewed as treating sentences or images as fully connected graphs where any word (or image patch) can attend to any other word in the sentence [12]. However, our input is a spatio-temporal graph skeleton of the human joint-bone structure with its own edge connectivity. Concatenating prompts along spatial or temporal dimensions would affect the graph semantics, and also affect standard training strategies such as a forward pass or backpropagation (especially in GCNs). Hence, we attach the selected prompts $\mathbf{P_T}$ to the corresponding input feature embedding $\mathbf{X_e}$ via a prompt attachment operator $f_p(.)$. The class logit distribution $\mathbf{y}$ is thus obtained as:

$$\mathbf{y} = f(\mathbf{X}, \mathbf{P_T}) = f_c \circ f_g \circ f_p(f_e(\mathbf{X}), \mathbf{P_T}) \tag{1}$$

In every user session $t > 0$, the classifier output dimension expands by N to accommodate the new action classes. Unlike most existing continual prompt tuning works, our feature extractor backbone f_g is trained only on the base class data $\mathcal{D}^{(0)}$ and is never fine-tuned on classes from new user sessions $\mathcal{US}^{(t)}, t > 0$. After the base session training, parameters of f_g, f_e are frozen.

Prompt Pool Design. As stated in Sec. 2.2, to encourage knowledge sharing across user sessions, we choose to construct a single prompt pool $\mathbf{P}$ which encodes

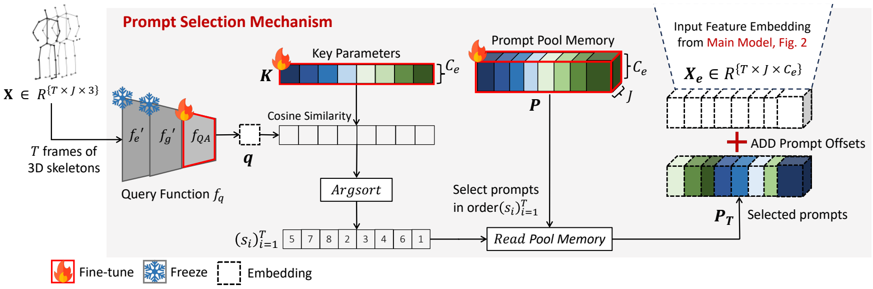

Fig. 3: **Selection of our prompts $\mathbf{P_T}$**: Input-dependent query $\boldsymbol{q}$ is matched with keys $\boldsymbol{K}$ using *sorted* cosine similarity to get an ordered index sequence $(s_i)_{i=1}^{T}$ of the top T keys. This ordered index sequence is used to select the corresponding ordered prompt sequence $\mathbf{P_T}$ from prompt pool $\mathbf{P}$. We *add* $\mathbf{P_T}$ to $\mathbf{X_e}$, thereby adding an offset to it. Our experimental evaluation confirms that such an additive spatio-temporal prompt offset can balance the plasticity to learn new classes from a few action samples, while maintaining stability on previously learned classes.

knowledge across the sessions:

$$\mathbf{P} = \{\boldsymbol{P_1}, ..\boldsymbol{P_i}, ..., \boldsymbol{P_M}\}, \qquad \boldsymbol{P_i} \in \mathbb{R}^{J \times C_e}; M = \#\text{prompts at time t} \tag{2}$$

For selecting prompts from this pool (Fig. 3), we construct a bijective key-value codebook, treating prompts in the pool $\mathbf{P}$ as values and defining learnable key vectors $\boldsymbol{K} = \{\boldsymbol{k_1}, .., \boldsymbol{k_i}, .., \boldsymbol{k_M}\}, \boldsymbol{k_i} \in \mathbb{R}^{C_e}$. A cosine similarity matching $\gamma(.)$ between the query $\boldsymbol{q}$ and keys $\boldsymbol{K}$ is used to find indices of the T closest keys $\mathbb{Z}$, which in turn are used to select prompts from the pool:

$$\mathbb{Z} = \underset{T}{\operatorname{argmax}}\, \gamma(f_q(\mathbf{X}), \boldsymbol{K}) \tag{3}$$

This quantization process is enabled by a query function $f_q(.)$, which is a pretrained encoder that maps an input instance $\mathbf{X}$ to a query $\boldsymbol{q}$ as:

$$\boldsymbol{q} = f_q(\mathbf{X}) = f_{QA} \circ f_g' \circ f_e'(\mathbf{X}), \qquad f_q : \mathbb{R}^{T \times J \times 3} \longrightarrow \mathbb{R}^{C_e} \tag{4}$$

where the *query adaptor* f_{QA} is a fully connected layer mapping the f_g' output dimension to the desired prompt embedding dimension C_e.

Coupled Optimization in User Sessions $t > 0$. Typically, the argmax operator in Eq. 3 decouples the optimization of keys from the prompt pool and main model as it prevents backpropagation of gradients to the keys (also seen in earlier works such as [48, 49]). However, this approach does not work for our setting, even more so since we assume no large-scale pre-training of our base model. Due to the lack of off-the-shelf availability of large-scale models for skeletal action data, our query function f_q is pretrained only on base class data $\mathcal{D}^{(0)}$. Hence, it becomes important that f_q is updated as the model learns new classes. As shown in red boxes in Figs. 2 and 3, we propose to couple this optimization process such that the overall cross-entropy loss for new tasks updates: (i) the classifier f_c, (ii) selected prompts in $\mathbf{P}$, (iii) selected keys in $\boldsymbol{K}$, as well as (iv) query adaptor f_{QA}. We achieve this by approximating the gradient for $\boldsymbol{K}$ and f_{QA} by the straight-through estimator reparameterization trick as in [3, 44]. We freeze the query feature extractor layers f_g', f_e' in $t > 0$ to prevent catastrophic forgetting of base knowledge in f_q. Our cross-entropy loss is hence given by:

$$\min_{\theta_{f_{QA}},\theta_{\boldsymbol{K}},\theta_{\mathbf{P}},\theta_{f_c}} \mathcal{L}(f(\mathbf{X},\mathbf{P_T}),\mathbf{y}) \tag{5}$$

To move queries closer to their aligned T keys during training, we use a vector quantization clustering loss inspired from VQ-VAE [44] as:

$$\max_{\theta_{f_{QA}},\theta_{\boldsymbol{K}}} \lambda \sum_{i\in\mathbb{Z}} \gamma(f_q(\mathbf{X}),\boldsymbol{K_i}) \tag{6}$$

where λ is the clustering loss coefficient. Our end-to-end optimization thus establishes a prompt optimization framework which is amenable to prompt tuning when extensive pre-training is not possible. This sets the foundation for our spatio-temporal prompt selection module, described next.

Spatio-Temporal Prompt Selection. In order to ensure that our learned prompts respect temporal information in the input video sequence, we choose the number of selected prompts to be equal to the number of frames in the input video T. After coupling the prompt pool and keys, we observed in our initial experiments with pool size $M > T$ that the same set of prompts get selected across training iterations and user sessions (Fig. 4A). More concretely, as the vector quantization loss (Eqn 6) brings the query close to the selected keys, the same set of active prompts get selected and optimized in each iteration, not using other prompts at all. This is similar to the well-known issue of '*codebook collapse*' in VQ-VAE [9, 50, 54]. Based on this observation, we design two prompt pool update mechanisms in user sessions $t > 0$ as below:

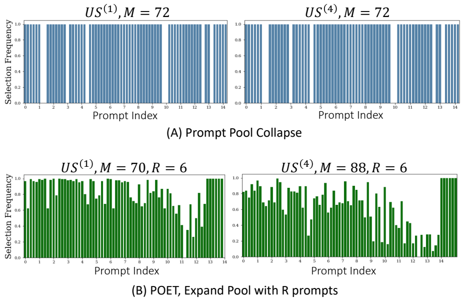

(A) Prompt Pool Collapse

(B) POET, Expand Pool with R prompts

Fig. 4: $M > T$ **Case: Prompt Pool Collapse.** (Top) Certain prompt indices remain unused across user sessions. (Bottom) Our POET pool expansion strategy alleviates pool collapse.

1. **Case 1,** $M = T \forall t$**:** *No pool expansion, Algorithm 1.* All prompts are selected in all tasks. But the *order of their selection* $(s_i)_{i=1}^T$ varies with each input instance as we replace Eq. 3 by sorting the cosine similarity before selecting the top T indices as follows:

$$\mathbb{Z} = \operatorname*{argsort}_{(s_i)_{i=1}^T} \gamma(f_q(\mathbf{X}),\boldsymbol{K}) \tag{7}$$

   In Fig. 5, we visualize the positions occupied by indices in this (sorted) *ordered key index sequence* $(s_i)_{i=1}^T$. Entropy increase across tasks $t = 1$ to $t = 4$ (bottom row of figure) shows that our selection mechanism learns to select a unique temporal code for all inputs.
2. **Case 2,** $M = T + (R * t), t > 0$**.** *Expand pool with R prompts.* We also propose an order-aware prompt pool expansion strategy (Appendix B) that selects prompts from an expanded pool in a temporally coherent manner, for $t > 0$. This alleviates prompt pool collapse as shown in Fig. 4B.

Prompt Offset Attachment. Since concatenation is not meaningful for graph data, we use addition as our choice for the prompt attachment operator as:

$$f_p(\mathbf{X_e}, \mathbf{P_T}) = \mathbf{X_e} + \mathbf{P_T} \tag{8}$$

Hence, we call our approach as *prompt offset tuning*. We also study this empirically through experiments that support this choice in Sec. 6.

Interpreting Prompt Offset Tuning of GNNs. Our additive prompt offsets are open to interpretation, as shown in Fig. 5. (i) Adding our selected prompts $\mathbf{P_T}$ to input feature embedding $\mathbf{X_e}$ acts like an input-dependent transformation for spatio-temporal joints. (ii) As our prompts have same size as $\mathbf{X_e}$, it can also be thought of as a learned prompt encoding, bearing similarity with learnable position encoding works [12, 24, 26]. Our purpose is different however as prompt offsets seek to dynamically condition the input for adapting the backbone continually, instead of learning positions. (iii) POET also bears similarity with auto-decoders like DeepSDF [30] which learn latent codes for each style or shape and use relevant codes along with a frozen decoder at inference. (iv) Prompt tuning can also be thought of as a *parameter isolation* technique for continual learning [28, 34, 35, 38]. POET's ordered prompt selection as seen in Fig. 5 learns to *isolate* the relevant sequence of prompts for each input action sequence.

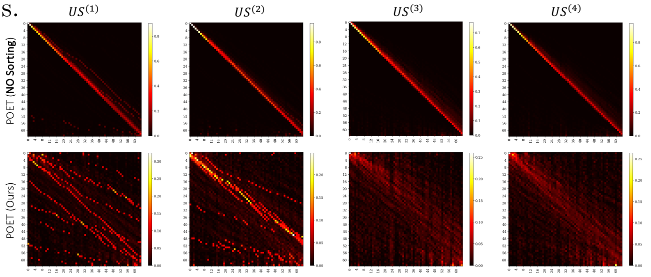

Fig. 5: Here we visualize the order $(s_i)_{i=1}^T$ in which the M = 64 **prompts in the pool are selected** at train time, across 4 user sessions $\mathcal{US}^{(t)}$. X-axis: prompt index, Y-axis: index position in selected sequence. *Top:* The no sorting case uses the default sequence (hence diagonal matrices), giving equal importance to all prompts. *Bottom (Our Method):* Even though the same 64 prompts are selected and updated, the ordering is temporally unique and consistent with input.

Algorithm 1 POET at Train Time, $t > 0$ (Case 1 $M = T$, No pool expansion)

```
Input: Query function $f_q$, keys $\boldsymbol{K} = \{\boldsymbol{k_j}\}_{j=1}^T$, prompt pool $\mathbf{P} = \{\boldsymbol{P_j}\}_{j=1}^T$; main model $f_e$, $f_g$, $f_c$
Initialize: $\mathbf{P}, \boldsymbol{K}$ from $t-1$; Expand $f_c$ by $N$ new classes. Initialize $f_c$ as: (i) copy $f_c^{old}$ weights, (ii) $f_c^{new} \leftarrow Mean(f_c^{old})$
Freeze: query layers $f_g', f_e'$; main model layers $f_e, f_g$
for epochs and batch $(\mathbf{X}_i^t, \mathbf{y}_i^t)_{i=1}^{NK}$ do
    1. Get query feature $\boldsymbol{q}$ (Eq. 4) ; Compute $\gamma(.)$ b/w query $\boldsymbol{q}$ and keys $\boldsymbol{K}$
    2. Sort $\gamma(.)$; Get ordered key index sequence $(s_i)_{i=1}^T$ (Eq. 7)
    3. Read pool memory $\mathbf{P}$ in order $(s_i)_{i=1}^T \rightarrow$ Get prompt offsets $\mathbf{P_T}$
    4. Get $\mathbf{X_e}$; Add $\mathbf{P_T}$ to it (Eq. 8); get prediction $\mathbf{y}$ from prompted input (Eq. 1)
    5. Use cross entropy loss (Equation 5) to update $f_{QA}, \boldsymbol{K}, \mathbf{P}, f_c$
    6. Use clustering loss (Equation 6) to update $f_{QA}$ and $\boldsymbol{K}$
end // See $t = 0$ training protocol in Algorithm 2 in Appendix
```

5 Experiments and Results

Datasets. We evaluated our method on well-known action recognition datasets[8]: (i) activity recognition on the NTU RGB+D dataset [39]; and (ii) hand gesture

[8] The datasets used in this work were accessed and processed at and by CMU. They were not accessed, processed, stored, or maintained at Meta.

recognition on the SHREC-2017 dataset [40]. As we introduce a new problem setting in human action recognition, we contribute two new benchmarks to the community for this setting, on the NTU RGB+D and SHREC-2017 datasets.

For the NTU RGB+D dataset, we divide the 60 daily action categories into 40 base classes, learning the remaining 20 classes in subsequent user sessions. In few-shot learning parlance, our protocol is 4-task 5-way 5-shot, i.e. 5 novel classes using 5 user training instances in 4 user sessions. Each input 3D skeleton sequence has 64 temporal frames, each consisting of 25 body keypoints, such that $x \in \mathcal{R}^{64\times25\times3}$. We use the spatio-temporal GCN, CTR-GCN [8], as the architecture for NTU RGB+D, where we choose the joint input modality for better interpretability of prompt tuning.

For SHREC-2017, we divide the 14 fine-grained hand gesture classes into 8 base classes and 6 classes learned in subsequent user sessions. This is done in a 3-task 2-way 5-shot protocol, i.e. 2 novel classes using 5 user training instances in 3 user sessions. For each input instance of SHREC-2017, we use 8 temporal frames each having 22 hand keypoints, such that input $x \in \mathcal{R}^{8\times22\times3}$. We use a fully-connected graph transformer backbone, DG-STA [7] for SHREC-2017. We select DG-STA due to easily reproducible code and to validate if our method POET works equally well across graph convolutional networks and graph transformers.

Evaluation Metrics. Following earlier work in similar settings [31], we report: (i) Average accuracy '*Avg*' of all classes seen so far, and (ii) Harmonic Mean A_{HM} between '*accuracy only on Old classes*' and '*accuracy only on New classes*' after learning each new user session. Note that the average accuracy tends to be biased towards the base session $\mathcal{T}^{(0)}$ performance due to more number of base classes. A higher A_{HM} implies better stability-plasticity trade-off between new task performance and old tasks' retention. Unlike many earlier CIL efforts, we report accuracy for both *Old* and *New* classes in each user session for transparency.

Implementation Details. We observe that a key source of forgetting in our setting is from the classifier as the logits tend to become heavily biased towards the few-shot samples of new classes. We use a cosine classifier for activity recognition experiments on CTR-GCN. For gesture recognition on the lightweight DG-STA, we use a standard fully-connected layer as classifier, but freeze old class parameters in the classifier by zeroing their gradients. We attach prompts after the 1st layer of DG-STA and 1st CTR-GC block of CTR-GCN. For both datasets, we have equal or higher learning rates in user sessions when compared to the base model's training in order to accommodate new knowledge in the model (for better plasticity). For exact implementation details (including learning rates, epochs, hyperparameter analysis, and backward forgetting metric), see Appendix A. In earlier efforts that more generally tune prompts for class-incremental learning [41, 45, 47–49], it is common to rely on an ImageNet21K pretrained ViT [37] or CLIP [33] as the backbone. However, such backbones do not exist for skeleton-based human action recognition. Our base feature extractor is hence trained on the base session dataset itself without *any* pretraining, making this one of the first efforts of prompt tuning without extensive pretraining (scale of data 3-5 times lower order of magnitude).

Results. Since there are no existing baselines for our proposed setting in skeletal action recognition, we compare our method by adapting continual learning (CL) baselines to skeletal data in Sec 5.1, Tables 1, 2. We first compare POET with prompt tuning based class-incremental learning (CIL) approaches originally designed for images (L2P [49], CODA-P [41], APT [4]) and find that it has very low performance on new classes as they do not update their query function. We find any fine-tuning or knowledge distillation based approaches (LWF [25], EWC [17], LUCIR [15]) lead to rapid forgetting of base knowledge as the model overfits to user's few-shots. We also compare with multiple variants of Feature Extraction (FE) to check if prompts truly have merit (POET=FE+Prompts) and provide upper bound baselines. In Sec 6, we first show the importance of prompts in POET by removing the prompts. We discuss the value of our coupled optimization, query function update and *ordered key index selection* in our prompt selection ablation Tab 3. We also study the impact of proposed additive prompt tuning as compared to other possible prompt attachments f_p in Tab 4.

5.1 Comparison with State-of-the-Art

POET sets the SOTA on existing prompt tuning works (Tab 1,2). We adapt three standard CIL works that prompt tune ViTs for images - L2P [49], CODA-P [41] and APT [4] to our setting. L2P and CODA-P share prompt pool across tasks (similar to us), whereas APT learns task-specific prompts. L2P decouples the optimization of keys from the prompt pool and concatenates the selected prompts. Since concatenation is not defined for our GNN backbone, we adapt these SOTA to our setting by concatenating along the temporal dimension (**L2P*, CODA-P***). CODA-P [41] couples keys with the prompt pool by using a cosine similarity weighing over all prompts in the pool, forming a 'soft prompt selection', different from our 'ordered hard prompt selection'. In **APT**, we train prompt-classifier pairs for each continual task separately ($\hat{}$ denotes task-specific), and use task identity at test time. See details in Appendix A. These methods by design rely on extensively pretrained (ImageNet21k) query functions which does not require updates; and require full supervision on new classes, perhaps explaining their poor 'New' accuracy in our few-shot setting.

Standard Continual learning Baselines. We compared with two well established knowledge-distillation approaches, learning without forgetting (**LWF**) and **LUCIR**. Both of them perform poorly on both old and new classes. **EWC** [17] learns better on new but does not retain old knowledge. We conclude that any CL method that fine-tunes the backbone feature representation in subsequent sessions $t > 0$ will not be able to retain base/old class knowledge (a finding consistent with existing FSCIL literature for images [10,43]). We also adapt and compare with one of the latest FSCIL baselines **ALICE** [31], originally developed for image classification benchmarks on our gesture recognition benchmark in Table 2. Note the high retention of base task performance (due to non-parametric classifier on top of frozen base model). However, it suffers from poor plasticity and adaptation to new classes. This is the issue of feature-classifier misalignment that we hoped to alleviate through prompt tuning.

Table 1: Activity Recognition Results (%, ↑), Comparison with SOTA: NTU RGB+D [39] dataset on CTR-GCN [8] backbone. After training on each incremental task, we report Average of all classes seen so far ('Avg'). We also report (i) A_{HM}, (ii) old classes accuracy ('Old'), (iii) new classes accuracy ('New') in the last session. We report Mean and STD across 10 sets of 5-shots. *POET achieves the best stability-plasticity trade-off across all baselines indicated by the* $A_{HM} = 56.3\%$. *POET also has the highest Avg across all user sessions outside of upper bound baselines in orange.*

	$\mathcal{UB}^{(0)}$	$\mathcal{US}^{(1)}$	$\mathcal{US}^{(2)}$	$\mathcal{US}^{(3)}$	$\mathcal{US}^{(4)}$			
Method	Base (↑)	Avg (↑)	Avg (↑)	Avg (↑)	Old (↑)	New (↑)	Avg (↑)	A_{HM} (↑)
Upper Bounds								
Joint (Oracle)	88.4	79.0	71.0	66.8			**63.5**	
Joint POET (Oracle)							**67.2**	
FE, Task-Specific^	88.4	70.1 ± 2.6	52.5 ± 5.8	44.8 ± 5.0	70.3 ± 2.1	46.7 ± 2.0	NA	NA
FE+Replay	88.4	82.4 ± 1.1	78.2 ± 1.2	74.5 ± 1.2	**73.1 ± 1.0**	43.3 ± 3.3	**70.6 ± 1.2**	54.3 ± 2.6
Continual Linear Probing								
FE	88.4	72.0 ± 1.1	60.4 ± 2.4	47.7 ± 2.1	40.0 ± 1.6	51.0 ± 2.3	40.9 ± 1.4	44.8 ± 1.1
FE, Frozen	88.4	76.1 ± 1.0	52.4 ± 4.1	38.3 ± 2.7	28.4 ± 1.6	22.4 ± 4.5	27.9 ± 1.4	24.8 ± 3.0
FE+Replay†	88.4	72.0 ± 1.5	59.5 ± 4.0	58.7 ± 2.8	56.7 ± 2.5	34.7 ± 5.6	54.9 ± 2.7	42.8 ± 4.4
FT	88.4	6.2 ± 1.4	4.3 ± 1.5	2.8 ± 1.0	0.2 ± 0.5	36.0 ± 10.1	3.2 ± 0.8	0.3 ± 1.0
Standard Continual Learning								
LWF [25]	88.4	6.2 ± 1.5	2.8 ± 0.7	3.7 ± 1.3	0.0 ± 0.0	38.9 ± 8.8	3.2 ± 0.7	0.0 ± 0.0
EWC [17]	88.4	6.6 ± 1.5	4.1 ± 1.4	3.1 ± 0.9	0.0 ± 0.0	42.1 ± 9.5	3.5 ± 0.8	0.0 ± 0.0
Experience Replay	88.4	35.1 ± 8.3	50.6 ± 5.0	60.6 ± 5.4	54.6 ± 6.5	43.7 ± 14.6	53.7 ± 7.1	47.8 ± 11.2
Experience Replay†	88.4	6.2 ± 1.5	9.0 ± 2.6	11.2 ± 3.0	10.9 ± 2.6	34.6 ± 7.9	12.9 ± 3.0	16.3 ± 3.5
LUCIR [15]	87.9	4.3 ± 2.1	4.1 ± 1.3	2.7 ± 0.8	0.2 ± 0.4	26.0 ± 9.2	2.3 ± 0.9	0.4 ± 0.8
Continual Prompt Tuning								
CODA-P [41]*	87.4	76.1 ± 1.0	66.7 ± 1.3	58.6 ± 2.7	56.5 ± 2.9	0.5 ± 0.4	51.8 ± 2.7	1.1 ± 0.7
L2P [49]*	88.6	78.9 ± 0.1	71.0 ± 1.0	64.2 ± 0.1	62.0 ± 0.7	0.0 ± 0.0	56.8 ± 0.6	0.0 ± 0.0
APT [4]^	86.6	27.3 ± 1.6	30.8 ± 3.4	37.6 ± 2.3	NA	33.4 ± 2.0	NA	NA
POET (Ours)	87.9	**82.3 ± 0.6**	**76.8 ± 0.9**	**68.4 ± 0.7**	**57.2 ± 1.0**	**55.8 ± 5.9**	**57.1 ± 1.1**	**56.3 ± 3.2**

Fine-tuning (FE) and Feature Extraction (FE) Baselines. We implement standard continual learning baselines to understand stability-plasticity trade-offs in our new benchmarks. In all these baselines, we expand the classifier output dimension by N new classes. In **'FT (Fine-Tuning)'**, we tune all model parameters on cross entropy loss of new task. FSCIL is challenging for this modality as old task performance sharply reduces to zero starting from $\mathcal{US}^{(1)}$ as model overfits to user's few-shots. **'FE (Feature Extraction)'**[9] differs from FT as we freeze the feature extractor to preserve base knowledge. This serves as a competitive baseline in our findings. In **'FE, frozen'**, we zero out the gradients of previous class weights in classifier f_c to prevent forgetting from the classifier. 'FE' and 'FE, Frozen' exhibit different New-Old trade-offs in Tables 1, 2 because the scale of pretraining is different (gesture more lightweight than activity).

Upper-bound baselines, top section Tables 1, 2. In **'Joint (oracle)'** experiment, we train on all task data at the same time in a multi-task (non-sequential) manner. Training POET in a multi-task manner (**'Joint POET'**) outperforms **'Joint Oracle'** demonstrating the strength of our approach. In addition to these *generalist* upper bounds, we point out that '**FE, Task-specific^**' is a competitive *specialist* upper bound. In this, we perform feature extraction from base model to each task individually, storing separate task-specific models ($\mathcal{US}^{(0)} \to \mathcal{US}^{(i)}$, $i > 0$). POET outperforms 'New' accuracy compared with this baseline, achieving a forward transfer on each $t > 0$. This indicates that prompt

[9] 'FE' is the same as 'w/o prompts' in Table 3. We highlight key baselines in gray color.

Table 2: Gesture Recognition Results (%, ↑), Comparison with SOTA: SHREC 2017 [40] dataset on DG-STA [7] graph transformer backbone. Reporting mean and standard deviation across 5 runs. **POET achieves best A_{HM} = 56.2%.**

	$\mathcal{UB}^{(0)}$	$\mathcal{US}^{(1)}$	$\mathcal{US}^{(2)}$	$\mathcal{US}^{(3)}$			
Method	Base (↑)	Avg (↑)	Avg (↑)	Old (↑)	New (↑)	Avg (↑)	A_{HM} (↑)
Joint (Oracle)	88.8	79.4 ± 0.7	77.3 ± 2.1			**70.9 ± 1.2**	**62.4 ± 0.4**
FT	88.8	20.3 ± 0.8	12.4 ± 2.1	0.0 ± 0.0	85.8 ± 9.4	13.4 ± 1.5	0.0 ± 0.0
FE	88.8	62.7 ± 2.4	41.9 ± 6.9	17.5 ± 5.1	77.3 ± 8.8	26.8 ± 3.4	28.5 ± 6.4
FE, Frozen	88.8	71.3 ± 1.9	61.4 ± 2.7	44.7 ± 3.2	54.5 ± 6.7	46.2 ± 2.7	49.1 ± 4.3
LWF [25]	88.8	20.2 ± 1.4	12.5 ± 1.0	0.0 ± 0.0	**88.4 ± 13.7**	13.8 ± 2.1	0.0 ± 0.0
L2P [49]**	88.8	20.3 ± 5.9	10.5 ± 4.8	8.2 ± 4.0	6.9 ± 8.5	7.9 ± 3.9	7.5 ± 5.5
CODA-P [41]**	87.7	15.6 ± 4.5	11.6 ± 1.9	7.9 ± 1.8	14.1 ± 21.4	8.8 ± 2.4	10.1 ± 3.2
ALICE [31]	92.1	72.4 ± 5.7	63.3 ± 7.6	**62.5 ± 6.8**	11.9 ± 9.9	**54.6 ± 6.9**	20.0 ± 8.1
POET (Ours)	91.9	73.2 ± 3.7	61.9 ± 1.8	45.9 ± 2.6	72.4 ± 7.1	50.0 ± 1.6	**56.2 ± 1.6**

tuning benefits New performance due to the pre-existing knowledge in the shared knowledge pool. Avg in sessions $0 < t < 4$ indicates New for task-specific^ .

Experience Replay Baselines, Tab 1. Even though our privacy-aware setting prohibits previous data replay, we compare with **'Experience Replay'** (store and replay 5-samples of base and incremental sessions) and **'Experience Replay†'** (replay only previous incremental sessions) for completeness. **'FE+Replay'** serves as the best upper bound (even better than Experience Replay as we are freezing backbone in addition to replay). It is noteworthy that POET (which is FE+prompts) learns an implicit 'data-free' form of prompt pool memory, and yet has a better A_{HM} trade-off as compared to explicitly stored and replayed samples from previous classes in FE+replay.

6 Ablation Studies and Analysis

Importance of prompts in POET. First, we *consider the contribution of prompt offsets in POET*. Since we only attach prompts to address continual learning in POET, removing prompts gives the Feature Extraction (FE) baseline ('w/o prompts', Table 3) where the backbone is frozen after base training and only the classifier is expanded and updated on classification loss of new classes. POET improves both, 'Old' (↑ 20.1%) and 'New' (↑ 10.6%) marked in blue.

Prompt Selection Mechanism. In Table 3, we investigate our prompt selection mechanism and optimization choices. The **'w/o coupled optim.'** experiment is a direct comparison of our additive *prompt attachment* with the de-coupled optimization in L2P [49]. Updating key parameters but keeping only query adaptor QA frozen after $\mathcal{UB}^{(0)}$ training (**'w/o QA update'**) reduces 'New' only performance of $\mathcal{US}^{(4)}$ by 4.6% as the query function stays fixed at base session learning and is not discriminative towards new classes. **'W/o clustering loss'** from Eq. 6, performance drops starting from $\mathcal{UB}^{(0)}$ itself. The only difference

Table 3: Prompt Selection Mechanism Analysis on NTU RGB+D dataset (%, ↑): 'w/o' denotes removing that component from POET, numbers in brackets are wrt *POET ($M = T$)* experiment. 'Avg' accuracy is biased towards 'Old' classes accuracy, A_{HM} is good indicator of trade-off between 'New' and 'Old'.

NTU RGB+D	$\mathcal{UB}^{(0)}$	$\mathcal{US}^{(1)}$	$\mathcal{US}^{(2)}$	$\mathcal{US}^{(3)}$	$\mathcal{US}^{(4)}$			
Method	Base	Avg	Avg	Avg	Old	New	Avg	A_{HM}
w/o prompts	88.4	74.5	66.3	49.5	39.2 (-20.1)	46.8 (-10.6)	39.9	42.7
w/o coupled optim.	88.0	82.8	75.3	65.8	56.5 (-2.8)	51.3 (-6.1)	56.1	53.8
w/o clustering loss	85.5	81.6	74.3	64.5	**62.0** (+2.7)	18.2 (-39.2)	57.0	28.1
w/o QA update	87.9	82.8	**77.4**	**69.1**	59.4 (+0.1)	52.8 (-4.6)	58.7	55.9
w/o sorting	88.2	82.2	75.2	68.8	59.9 (+0.6)	46.6 (-10.8)	58.8	52.4
POET ($M > T$)	87.9	82.7	77.2	68.8	60.3 (+1.0)	54.4 (-3.0)	**59.8**	57.2
POET ($M = T$)	87.9	**82.8**	76.8	68.6	59.3	**57.4**	**59.2**	**58.3**

between the experiment **‘w/o sorting’** and ‘POET (M=T)’ is that we do not *sort* the cosine similarity before selecting top T indices (same as Fig 5). The 10.8% ↑ in ‘New’ performance validates that our prompt selection mechanism is learning to chose a distinct temporal ordering for prompt tuning of new input samples. With pool expansion (**‘POET, $M > T$’**), we get more flexibility in the stability-plasticity trade-offs depending on how many new prompts we attach. For $R = 6$, ‘Old’ is improved. In Table 3, we keep POET’s additive prompt attachment and only vary prompt selection.

Prompt Attachment Mechanism. In Table 4, we keep our end-to-end optimization and ordered prompt selection as a constant and ablate prompt shape and attachment operator $f_p(.)$. Drawing a parallel with transformers which concatenate prompts along the token dimension, we conduct experiments concatenating prompts along the (i) temporal dimension of the skeleton input feature embedding $\mathbf{X_e}$ (*‘CONCAT temporal’*) and (ii) feature dimension C_e (*‘CONCAT feature’*). We find that addition works better than concatenation and cross attention. We also verify our hypothesis that selecting the same number of prompts as the input temporal dimension ($T = 64$ for NTU RGB+D and $T = 8$ for SHREC-2017) yields better results as compared to adding the same prompt frame to each input embedding frame (*‘Addition $T' = 1$’*).

Table 4: Prompt Attachment Analysis (%, ↑): The best prompt attachment choice $f_p(.)$ is *Adding* #prompts same as #input frames (T=64).

NTU RGB+D	$\mathcal{UB}^{(0)}$	$\mathcal{US}^{(1)}$	$\mathcal{US}^{(2)}$	$\mathcal{US}^{(3)}$	$\mathcal{US}^{(4)}$			
Method	Base	Avg	Avg	Avg	Old	New	Avg	A_{HM}
CONCAT temporal, $T' = 64$	88.6	70.3	62.4	49.8	33.6	50.5	35.1	40.3
CONCAT feature, $T' = 64$	87.7	82.4	75.5	66.9	57.1	41.5	56.0	48.1
Cross Attention, $T' = 64$	82.9	77.4	72.2	65.0	57.1	32.3	55.0	41.2
ADD, $T' = 1$	**88.7**	73.3	62.7	45.5	33.7	47.0	34.8	39.3
ADD, $T' = 64$ (Ours)	87.9	**82.8**	**76.8**	**68.6**	59.3	**57.4**	59.2	**58.3**

7 Conclusions and Future Work

The problem of continually adapting human action models to new user categories over time has gained prominence with the rising availability of XR devices. However, this setting poses unique challenges: (i) the user may be able to provide only a few samples for training, and (ii) accessing data from earlier sessions may violate privacy considerations. We hence propose a method based on prompt offset tuning to address this problem in this work. Prompt tuning to address learning over newer tasks has been attempted in recent years. However, these works have: (1) typically been designed for image-based tasks, (2) relied on strongly pretrained transformer backbones, (3) required full supervision for new tasks, and (4) exclusively applied prompt tuning to transformer architectures. This work departs from these four characteristics. Our work demonstrates that prompt offset tuning is a promising option to evolve and adapt skeleton-based human action models to new user classes. The careful design of each component of the proposed methodology finds validation in the promising results across well-known skeleton-based action recognition benchmarks. Our ablation studies and analysis corroborate our design choices in our implementation. Looking ahead, it will be interesting to explore how our approach and its design choices adapt when a “generalist backbone" trained on a large corpus of action recognition data becomes accessible. Extending our method for differential privacy is another interesting direction of future work.

References

1. Aich, S., Ruiz-Santaquiteria, J., Lu, Z., Garg, P., Joseph, K.J., Fernandez, A., Balasubramanian, V.N., Kin, K., Wan, C., Camgoz, N.C., Ma, S., De la Torre, F.: Data-free class-incremental hand gesture recognition. In: Proceedings of the IEEE/CVF International Conference on Computer Vision (2023)
2. Albrecht, J.P.: How the gdpr will change the world. Eur. Data Prot. L. Rev. **2**, 287 (2016)
3. Bengio, Y., Léonard, N., Courville, A.: Estimating or propagating gradients through stochastic neurons for conditional computation. arXiv preprint arXiv:1308.3432 (2013)
4. Bowman, B., Achille, A., Zancato, L., Trager, M., Perera, P., Paolini, G., Soatto, S.: a-la-carte prompt tuning (apt): Combining distinct data via composable prompting. In: Proceedings of the IEEE/CVF Conference on Computer Vision and Pattern Recognition. pp. 14984–14993 (2023)
5. Chaudhry, A., Dokania, P.K., Ajanthan, T., Torr, P.H.: Riemannian walk for incremental learning: Understanding forgetting and intransigence. In: Proceedings of the European conference on computer vision (ECCV). pp. 532–547 (2018)
6. Chaudhry, A., Ranzato, M., Rohrbach, M., Elhoseiny, M.: Efficient lifelong learning with a-gem. arXiv preprint arXiv:1812.00420 (2018)
7. Chen, Y., Zhao, L., Peng, X., Yuan, J., Metaxas, D.N.: Construct dynamic graphs for hand gesture recognition via spatial-temporal attention. In: Proceedings of the British Machine Vision Conference (BMVC) (2019)
8. Chen, Y., Zhang, Z., Yuan, C., Li, B., Deng, Y., Hu, W.: Channel-wise topology refinement graph convolution for skeleton-based action recognition. In: Proceedings of the IEEE/CVF International Conference on Computer Vision. pp. 13359–13368 (2021)
9. Dhariwal, P., Jun, H., Payne, C., Kim, J.W., Radford, A., Sutskever, I.: Jukebox: A generative model for music. arXiv preprint arXiv:2005.00341 (2020)
10. Dong, S., Hong, X., Tao, X., Chang, X., Wei, X., Gong, Y.: Few-shot class-incremental learning via relation knowledge distillation. In: Proceedings of the AAAI Conference on Artificial Intelligence. vol. 35, pp. 1255–1263 (2021)
11. Dwivedi, V.P., Bresson, X.: A generalization of transformer networks to graphs. arXiv preprint arXiv:2012.09699 (2020)
12. Dwivedi, V.P., Luu, A.T., Laurent, T., Bengio, Y., Bresson, X.: Graph neural networks with learnable structural and positional representations. In: International Conference on Learning Representations (2022), https://openreview.net/forum?id=wTTjnvGphYj
13. Hersche, M., Karunaratne, G., Cherubini, G., Benini, L., Sebastian, A., Rahimi, A.: Constrained few-shot class-incremental learning. In: Proceedings of the IEEE/CVF Conference on Computer Vision and Pattern Recognition. pp. 9057–9067 (2022)
14. Hinojosa, C., Marquez, M., Arguello, H., Adeli, E., Fei-Fei, L., Niebles, J.C.: Privhar: Recognizing human actions from privacy-preserving lens. In: European Conference on Computer Vision. pp. 314–332. Springer (2022)
15. Hou, S., Pan, X., Loy, C.C., Wang, Z., Lin, D.: Learning a unified classifier incrementally via rebalancing. In: Proceedings of the IEEE/CVF conference on computer vision and pattern recognition. pp. 831–839 (2019)
16. Jia, M., Tang, L., Chen, B.C., Cardie, C., Belongie, S., Hariharan, B., Lim, S.N.: Visual prompt tuning. In: European Conference on Computer Vision. pp. 709–727. Springer (2022)

17. Kirkpatrick, J., Pascanu, R., Rabinowitz, N., Veness, J., Desjardins, G., Rusu, A.A., Milan, K., Quan, J., Ramalho, T., Grabska-Barwinska, A., et al.: Overcoming catastrophic forgetting in neural networks. Proceedings of the national academy of sciences **114**(13), 3521–3526 (2017)
18. Kumawat, S., Nagahara, H.: Privacy-preserving action recognition via motion difference quantization. In: European Conference on Computer Vision. pp. 518–534. Springer (2022)
19. Lacoste, A., Luccioni, A., Schmidt, V., Dandres, T.: Quantifying the carbon emissions of machine learning. arXiv preprint arXiv:1910.09700 (2019)
20. Lester, B., Al-Rfou, R., Constant, N.: The power of scale for parameter-efficient prompt tuning. arXiv preprint arXiv:2104.08691 (2021)
21. Li, M., Xu, X., Fan, H., Zhou, P., Liu, J., Liu, J.W., Li, J., Keppo, J., Shou, M.Z., Yan, S.: Stprivacy: Spatio-temporal privacy-preserving action recognition. In: Proceedings of the IEEE/CVF International Conference on Computer Vision. pp. 5106–5115 (2023)
22. Li, T., Ke, Q., Rahmani, H., Ho, R.E., Ding, H., Liu, J.: Else-net: Elastic semantic network for continual action recognition from skeleton data. In: Proceedings of the IEEE/CVF International Conference on Computer Vision. pp. 13434–13443 (2021)
23. Li, X.L., Liang, P.: Prefix-tuning: Optimizing continuous prompts for generation. arXiv preprint arXiv:2101.00190 (2021)
24. Li, Y., Si, S., Li, G., Hsieh, C.J., Bengio, S.: Learnable fourier features for multidimensional spatial positional encoding. Advances in Neural Information Processing Systems **34**, 15816–15829 (2021)
25. Li, Z., Hoiem, D.: Learning without forgetting. IEEE transactions on pattern analysis and machine intelligence **40**(12), 2935–2947 (2017)
26. Liu, X., Yu, H.F., Dhillon, I., Hsieh, C.J.: Learning to encode position for transformer with continuous dynamical model. In: International conference on machine learning. pp. 6327–6335. PMLR (2020)
27. Ma, N., Zhang, H., Li, X., Zhou, S., Zhang, Z., Wen, J., Li, H., Gu, J., Bu, J.: Learning spatial-preserved skeleton representations for few-shot action recognition. In: European Conference on Computer Vision. pp. 174–191. Springer (2022)
28. Mallya, A., Lazebnik, S.: Packnet: Adding multiple tasks to a single network by iterative pruning. In: Proceedings of the IEEE conference on Computer Vision and Pattern Recognition. pp. 7765–7773 (2018)
29. Mialon, G., Chen, D., Selosse, M., Mairal, J.: Graphit: Encoding graph structure in transformers. arXiv preprint arXiv:2106.05667 (2021)
30. Park, J.J., Florence, P., Straub, J., Newcombe, R., Lovegrove, S.: Deepsdf: Learning continuous signed distance functions for shape representation. In: Proceedings of the IEEE/CVF conference on computer vision and pattern recognition. pp. 165–174 (2019)
31. Peng, C., Zhao, K., Wang, T., Li, M., Lovell, B.C.: Few-shot class-incremental learning from an open-set perspective. In: European Conference on Computer Vision. pp. 382–397. Springer (2022)
32. Pernici, F., Bruni, M., Baecchi, C., Turchini, F., Del Bimbo, A.: Class-incremental learning with pre-allocated fixed classifiers. In: 2020 25th International Conference on Pattern Recognition (ICPR). pp. 6259–6266. IEEE (2021)
33. Radford, A., Kim, J.W., Hallacy, C., Ramesh, A., Goh, G., Agarwal, S., Sastry, G., Askell, A., Mishkin, P., Clark, J., et al.: Learning transferable visual models from natural language supervision. In: International conference on machine learning. pp. 8748–8763. PMLR (2021)

34. Razdaibiedina, A., Mao, Y., Hou, R., Khabsa, M., Lewis, M., Almahairi, A.: Progressive prompts: Continual learning for language models. arXiv preprint arXiv:2301.12314 (2023)
35. Rebuffi, S.A., Bilen, H., Vedaldi, A.: Efficient parametrization of multi-domain deep neural networks. In: Proceedings of the IEEE conference on computer vision and pattern recognition. pp. 8119–8127 (2018)
36. Ren, B., Liu, M., Ding, R., Liu, H.: A survey on 3d skeleton-based action recognition using learning method. Cyborg and Bionic Systems (2020)
37. Ridnik, T., Ben-Baruch, E., Noy, A., Zelnik-Manor, L.: Imagenet-21k pretraining for the masses. arXiv preprint arXiv:2104.10972 (2021)
38. Rusu, A.A., Rabinowitz, N.C., Desjardins, G., Soyer, H., Kirkpatrick, J., Kavukcuoglu, K., Pascanu, R., Hadsell, R.: Progressive neural networks. arXiv preprint arXiv:1606.04671 (2016)
39. Shahroudy, A., Liu, J., Ng, T.T., Wang, G.: Ntu rgb+ d: A large scale dataset for 3d human activity analysis. In: Proceedings of the IEEE conference on computer vision and pattern recognition. pp. 1010–1019 (2016)
40. Smedt, Q.D., Wannous, H., Vandeborre, J.P., Guerry, J., Saux, B.L., Filliat, D.: 3D Hand Gesture Recognition Using a Depth and Skeletal Dataset. In: Pratikakis, I., Dupont, F., Ovsjanikov, M. (eds.) Eurographics Workshop on 3D Object Retrieval. The Eurographics Association (2017). https://doi.org/10.2312/3dor.20171049
41. Smith, J.S., Karlinsky, L., Gutta, V., Cascante-Bonilla, P., Kim, D., Arbelle, A., Panda, R., Feris, R., Kira, Z.: Coda-prompt: Continual decomposed attention-based prompting for rehearsal-free continual learning. In: Proceedings of the IEEE/CVF Conference on Computer Vision and Pattern Recognition. pp. 11909–11919 (2023)
42. Tang, Y.M., Peng, Y.X., Zheng, W.S.: When prompt-based incremental learning does not meet strong pretraining. arXiv preprint arXiv:2308.10445 (2023)
43. Tao, X., Hong, X., Chang, X., Dong, S., Wei, X., Gong, Y.: Few-shot class-incremental learning. In: Proceedings of the IEEE/CVF Conference on Computer Vision and Pattern Recognition. pp. 12183–12192 (2020)
44. Van Den Oord, A., Vinyals, O., et al.: Neural discrete representation learning. Advances in neural information processing systems **30** (2017)
45. Villa, A., Alcázar, J.L., Alfarra, M., Alhamoud, K., Hurtado, J., Heilbron, F.C., Soto, A., Ghanem, B.: Pivot: Prompting for video continual learning. In: Proceedings of the IEEE/CVF Conference on Computer Vision and Pattern Recognition. pp. 24214–24223 (2023)
46. Wang, X., Zhang, S., Qing, Z., Gao, C., Zhang, Y., Zhao, D., Sang, N.: Molo: Motion-augmented long-short contrastive learning for few-shot action recognition. In: Proceedings of the IEEE/CVF Conference on Computer Vision and Pattern Recognition. pp. 18011–18021 (2023)
47. Wang, Y., Huang, Z., Hong, X.: S-prompts learning with pre-trained transformers: An occam's razor for domain incremental learning. Advances in Neural Information Processing Systems **35**, 5682–5695 (2022)
48. Wang, Z., Zhang, Z., Ebrahimi, S., Sun, R., Zhang, H., Lee, C.Y., Ren, X., Su, G., Perot, V., Dy, J., et al.: Dualprompt: Complementary prompting for rehearsal-free continual learning. In: European Conference on Computer Vision. pp. 631–648. Springer (2022)
49. Wang, Z., Zhang, Z., Lee, C.Y., Zhang, H., Sun, R., Ren, X., Su, G., Perot, V., Dy, J., Pfister, T.: Learning to prompt for continual learning. In: Proceedings of the IEEE/CVF Conference on Computer Vision and Pattern Recognition. pp. 139–149 (2022)

50. Williams, W., Ringer, S., Ash, T., MacLeod, D., Dougherty, J., Hughes, J.: Hierarchical quantized autoencoders. Advances in Neural Information Processing Systems **33**, 4524–4535 (2020)
51. Yang, Y., Yuan, H., Li, X., Lin, Z., Torr, P., Tao, D.: Neural collapse inspired feature-classifier alignment for few-shot class-incremental learning. In: The Eleventh International Conference on Learning Representations (2023), https://openreview.net/forum?id=y5W8tpojhtJ
52. Yue, R., Tian, Z., Du, S.: Action recognition based on rgb and skeleton data sets: A survey. Neurocomputing (2022)
53. Zhang, H.B., Zhang, Y.X., Zhong, B., Lei, Q., Yang, L., Du, J.X., Chen, D.S.: A comprehensive survey of vision-based human action recognition methods. Sensors **19**(5), 1005 (2019)
54. Zheng, C., Vedaldi, A.: Online clustered codebook. In: Proceedings of the IEEE/CVF International Conference on Computer Vision. pp. 22798–22807 (2023)
55. Zhou, D.W., Wang, F.Y., Ye, H.J., Ma, L., Pu, S., Zhan, D.C.: Forward compatible few-shot class-incremental learning. In: Proceedings of the IEEE/CVF conference on computer vision and pattern recognition. pp. 9046–9056 (2022)
56. Zhu, A., Ke, Q., Gong, M., Bailey, J.: Adaptive local-component-aware graph convolutional network for one-shot skeleton-based action recognition. In: Proceedings of the IEEE/CVF Winter Conference on Applications of Computer Vision. pp. 6038–6047 (2023)
57. Zhu, B., Niu, Y., Han, Y., Wu, Y., Zhang, H.: Prompt-aligned gradient for prompt tuning. In: Proceedings of the IEEE/CVF International Conference on Computer Vision. pp. 15659–15669 (2023)